

Identification and Localization of Cometary Activity in Solar System Objects with Machine Learning

Bryce T. Bolin

*organization=Goddard Space Flight Center,addressline=8800 Greenbelt Road,
city=Greenbelt, postcode=20771, state=MD, country=USA*

Michael W. Coughlin

*organization=School of Physics and Astronomy, University of
Minnesota,addressline=116 Church St SE, city=Twin Cities, postcode=55455,
state=MN, country=USA*

Abstract

In this chapter, we will discuss the use of Machine Learning methods for the identification and localization of cometary activity for Solar System objects in ground and in space-based wide-field all-sky surveys. We will begin the chapter by discussing the challenges of identifying known and unknown active, extended Solar System objects in the presence of stellar-type sources and the application of classical pre-ML identification techniques and their limitations. We will then transition to the discussion of implementing ML techniques to address the challenge of extended object identification. We will finish with prospective future methods and the application to future surveys such as the Vera C. Rubin Observatory.

Key words: Minor planets, asteroids: general, Minor planets, asteroids: individual, Machine learning, Neural Networks, comet and asteroid identification, minor planet surveys.

1. Introduction to the identification of cometary activity in Solar System objects

Current and next-generation all-sky surveys provide unprecedented opportunities for the discovery of solar system asteroids and comets (Jedicke et al., 2016; Bauer et al., 2022). Contemporary asteroid surveys employ a

variety of algorithms and pipelines to detect and identify moving objects in their image data such as the association of two or more detections taken in a sequence called “tracklets” (e.g. Jedicke et al., 2015) or through the shifting and stacking of multiple images together (e.g. Whidden et al., 2019; Bolin et al., 2020). This involves taking multiple images to detect an object more than once within a short enough time for the detections to be linked. The actual linkage of detection can include decision trees or the connection of several detections together within similar co-moving velocities (Kubica et al., 2005; Masci et al., 2019).

Multiple detection linking algorithms can link the detections of both point-source, asteroidal detections and those that are extended, as for comets. Even for comets, whose detections have a large, extended appearance, multiple detections can be linked as for point sources if the measurement of the comet’s position relative to the moving frame of the object is consistent from detection to detection (Denneau et al., 2013). However, in some survey imaging pipelines, extended objects, defined as having a width more expansive than the measured width for known point sources, can be flagged as potential outliers and removed from further processing (Duez et al., 2019). The similarities between extended objects and common telescope/detector artifacts can cause the source detection pipeline to fail; therefore, the flagging and removal of extended objects can be motivated by the need to keep the false positives at manageable levels for vetting by human eyes. As a result, the detection and discovery of comets by all-sky surveys can depend not only on the ability of the algorithms to link the detection of comets from multiple images but also on the base level of extraction of detections on a per-image basis.

The ability to detect comets can vary from survey to survey due to the ability to detect extended objects. For example, the image processing pipeline for the ZTF survey rejects extended objects due to the contamination of artifacts (Masci et al., 2019). Therefore, the detection of comets is significantly limited in surveys such as ZTF using the standard data pipeline. Furthermore, the ability to link comet detections can be substantially different than the detection and linking of asteroidal or point-source-like detections. The detection and discovery of comets may require their detection to be non-extended to avoid being flagged as an artifact. Examples of such cases are where the appearance of a comet is non-extended, either by its extent not being detectable given the seeing conditions at the observing location of the survey (typically 1-2 arcseconds Jedicke et al., 2015) or by being dis-

covered as a bare nucleus before their activity starts (e.g., Cheng and Wu, 2022). In this review chapter, we will focus on identifying comets as truly extended sources, i.e., that have morphological features that are recognized as extended at the resolution of the survey. We will describe classical methods of identifying comets in astronomical survey data as well as by follow-up data. We will also describe recent advances in machine learning techniques applied to observations of comets that assist in their recognition as extended cometary sources versus being asteroidal, focusing on advancements in Deep Learning. Lastly, we will describe techniques that are being mastered for near-future use for the detection and discovery of comets in astronomical surveys such as the forthcoming Vera C. Rubin Observatory’s Legacy Survey of Space and Time (LSST, Schwamb et al., 2023).

2. Review of classical comet detection methods and strategies

We will start this review with an overview of contemporary methods for finding comets in astronomical surveys and follow-up data. We will start this section with a brief discussion of ”classical” comet detection methods, i.e., those not based on machine learning or Deep Learning methods. We refer to these methods as classical since they were, in principle, accessible before the wide-scale adoption of computational methods in astronomy, i.e., when the discovery of comets occurred by recognition of an extended object by the human eye (Festou et al., 1993). However, for this review, we set a lower bound to the time covered by classical comet identification methods to the early to late 1990s when consumer-grade charge-coupled devices (CCDs) became widely accessible for use in astronomical surveys. We will transition from classical methods to methods based on characterizing individual detections to data science and machine learning-driven methods, which became more prevalent in the 2010s.

2.1. *Serendipitous identification of cometary activity of unknown objects*

The first discovery of a comet as an unknown object with an automated asteroid detection pipeline was made in 1992 of C/1992 J1 (Spacewatch) by the Spacewatch survey (Scotti et al., 1992). Spacewatch was one of the first surveys to use an automated pipeline for the detection of asteroids in CCD observations, while the telescope was used in drift scan mode (Jedicke et al., 2015). Several asteroid surveys using CCD technology began after Spacewatch such as the Catalina Sky Survey, Lincoln Near-Earth

Asteroid Research, Panoramic Survey Telescope and Rapid Response System (Pan-STARRS) (Chambers et al., 2016), the Near-Earth Object Wide-field Infrared Survey Explorer (NEOWISE) (Mainzer et al., 2011), Asteroid Terrestrial-impact Last Alert System (ATLAS) (Tonry et al., 2018), and the Zwicky Transient Facility (ZTF) (Bellm et al., 2019) (for a review of asteroid surveys, please see Jedicke et al., 2015). These ground and space-based surveys discovered numerous comets, ~ 1000 by the end of the 2020s (Bauer et al., 2022). The SOHO and STEREO observatories also discovered several thousand comets as they passed near the Sun in the field of view of these spacecraft (for an overview, please see Battams and Knight, 2017). However, for this review, we will focus on comet discoveries made by asteroid-dedicated surveys.

2.2. Identification of cometary activity in known objects

As described above, the discovery of cometary activity can be decoupled from the initial recognition of a solar system object, i.e., it will be recognized as a candidate asteroid detection agnostic of its activity. A known candidate orbit is the main product of a series of observations of an asteroid candidate. Even if the detection of a candidate comet’s activity is not known, the orbit resulting from the observations can provide clues as to its cometary nature. A clue to the cometary nature of a comet candidate can be deduced from the known orbit such as having a Tisserand parameter significantly less than 3 (for a review of the Tisserand parameter and its significance to comets, please see Fraser et al., 2022). In addition, having an eccentricity of $\gtrsim 1$ or retrograde inclination may suggest that an asteroidal object has a cometary origin versus an asteroidal one. This is because most observed asteroids, such as those in the Main Belt, have an eccentricity less than 0.3 and an inclination less than 17 degrees (e.g., Bolin et al., 2017, 2018)

Comets which from their orbital properties provide clues of cometary origins may encourage follow-observations that are deeper in limiting magnitude and sensitivity which may result in the detection of cometary activity. A recent example is in the discovery of C/2022 E (ZTF) (Bolin et al., 2022b) which, while possessing evident activity in subsequent observations, had an asteroidal appearance in the discovery images taken by ZTF. Subsequent observations taken by amateur astronomers specializing in the follow-up of comets, as well as in subsequent observations by ZTF, showed evidence of cometary activity in the form of a tail and coma (Sato et al., 2022; Bolin et al., 2024b, , Fig. 1). Clues to its cometary origin, which inspired follow-up

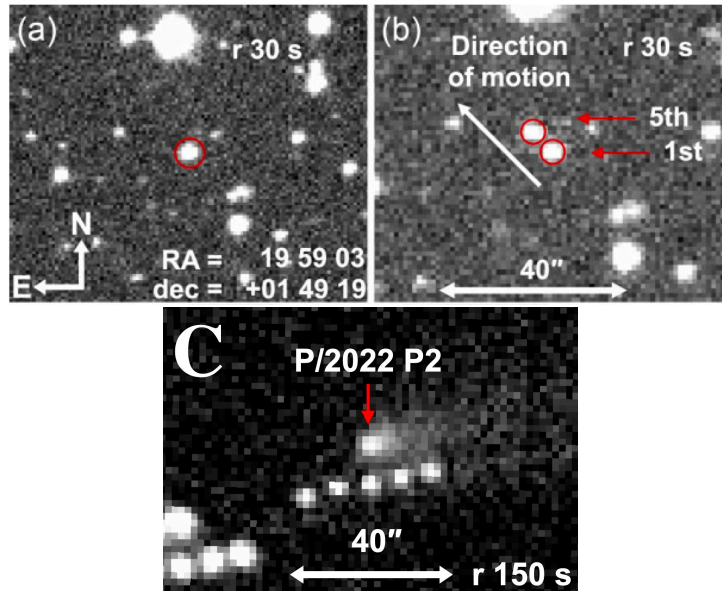


Figure 1: Discovery images of C/2022 E3 (ZTF) taken by ZTF in 2022 March. The top panel shows one of the individual detections of the comet (taken in a series of 5). The top right panel shows a composite stack of the first and fifth images stacked on the background stars. The bottom panel shows a composite stack of all five images co-added together. The exposure time, filter, and cardinal directions are indicated. Adapted from Figure 1 of Bolin et al. (2024b) and reproduced with the permission of the authors and MNRAS. The bottom panel shows a co-added composite stack of all five 30 s exposures of images of comet P/2022 P2 (ZTF) taken by ZTF in 2022 August (Bolin et al., 2024a).

observations, came from its eccentricity of ~ 1 and retrograde inclination of ~ 109 degrees, typical for long-period comets and distinct from the population of asteroids (Jedicke et al., 2002; Gladman et al., 2008; Nesvorný et al., 2023).

3. Review of cometary detections methods based on measurements of the individual detections

Next, we discuss detecting cometary activity by inspecting objects on an individual image basis. Previous techniques relied on identifying comets following the linkage of multiple detections of objects taken in multiple images. The next set of techniques relies on the previous knowledge of the location of a known object in CCD images and inspects each detection individually.

Thus, the detection of cometary activity can be done with individual images instead of grouped images.

3.1. Identification of comets through spread function parameter analysis

Extended objects in astronomical images, whether in-ground or space-based observations, are defined by their extent relative to the typical width of unresolved detections. In images taken by single-dish telescopes, the width of the point spread function (PSF), the detection of a point or unresolved source, is set by the diffraction limits of the telescope optics, directly proportional to the observed wavelength and inversely proportional to the diameter of the telescope (Born and Wolf, 1999). In CCD detections, the PSF can be super-sampled, that is, when the scale of the individual pixels is less than the critical sample rate, and sub-sampled if the pixel scale is larger than the critical sampled rate (Howell, 2000).

Detecting extended cometary features such as a tail or coma depends on their angular size, which is significantly larger than the imager’s resolution. Even when observing with a telescope that enables resolving objects at a diffraction limit smaller than the angular scale of an extended comet, the extendedness may not be resolved if the effective resolution of the images is too coarse due to pixel size. Additionally, the resolution is often limited by the quality of atmospheric seeing when observing from the ground (typically ~ 1 arcsecond at most professional observing sites) rather than being limited by the inherent diffraction limit of the telescope’s optics.

Several attempts have been made to identify comets by quantification of the quality and extendedness of their PSFs. The quality of a PSF is roughly indicated by the reliability of PSF shape measurements made of asteroid detections by imaging pipelines (e.g., as for Pan-STARRS, see Chambers et al., 2016). For the identification of comet candidates, the measured size of the PDF is compared to the expected PSF size for a non-resolved, point-like source. Active comet candidates are more likely to have PSFs that are significantly more extended than compared to stellar-like sources (top panel of Fig. 2). Studies of the detection of comets at Palomar observatory and with Pan-STARRS found a significant correlation between parameters describing the extent and quality of PSF for comets when compared to asteroidal detections (see Fig. 2) (Waszczak et al., 2013; Hsieh et al., 2015). This method resulted in the discovery of numerous comets with Pan-STARRS, including several Main Belt comets/Active asteroids (e.g., Bolin et al., 2013; Hill et al., 2013).

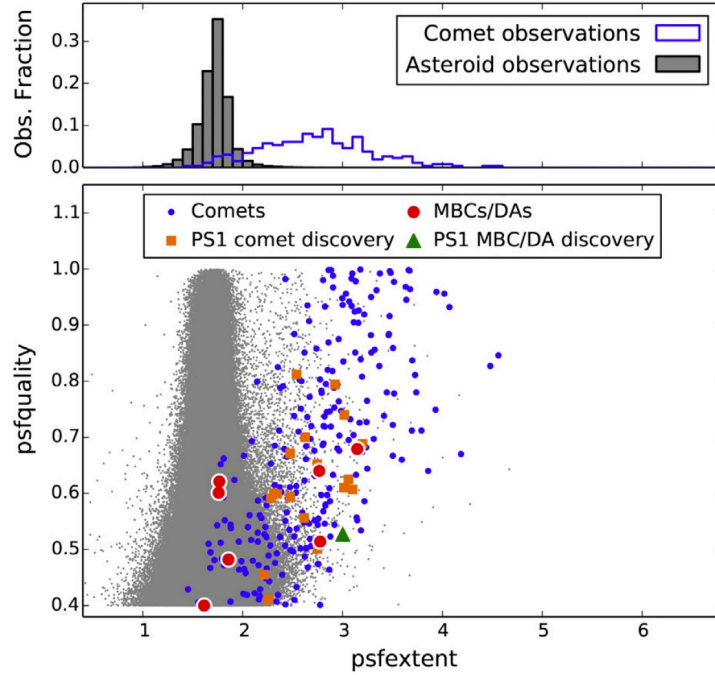


Figure 2: Comparison of the PSF extent, psfextent , and PSF quality, psfquality , properties of asteroid and comet detections from Pan-STARRS taken before 2013 July. psfextent refers to the extendedness of detection PSFs measured as the full width at half maximum of the PSF in arcseconds compared to the expected PSF of point sources. Higher values of psfextent correspond to sources being more extended. psfquality refers to the reliability of PSF measurements with a higher number being more favorable. Top panel: 1-D histograms of PSF extent of asteroid detections (grey) and comet detections (blue). Bottom panel: 2-D distribution of psfextent vs psfquality . The psfextent and psfquality for asteroids is in grey, comets in blue/orange, and Main Belt comets/active asteroids in red and green. Adapted from Figure 5 of Hsieh et al. (2015) and reproduced with the permission of the authors and Icarus. We refer readers to the asteroid and comet detection gallery seen in Fig. 18 of Denneau et al. (2013) for examples of asteroidal and extended comet detections.

3.2. Identification of cometary activity by detection of comae and azimuthal variations

While the PSF extendedness method provides a straightforward and intuitive method for flagging comet candidates by their candidate extendedness when compared to reference point-source PSFs, this comparison is not based on the observed attributes of comets. Comets that can have azimuthal asymmetry due to the presence of tails or a central extended compact coma that may not be easily represented by a PSF (e.g., Bolin and Lisse, 2020; Bolin et al., 2021). Improvements to searching for cometary signatures in candidate comet detections can be made by searching for azimuthal asymmetry and the presence of a coma with special aperture functions designed to detect these properties.

Sonnett et al. (2011) were the first to apply the azimuthal asymmetry and coma search technique to ~ 1000 asteroids detected by the Thousand Asteroid Lightcurve Survey taken with the Canada France Hawaii Telescope (Masiero et al., 2009). They used a scheme shown in Fig. 3 that divides an annulus outside the extent of the central coma into 18 sections. The section containing part(s) of a candidate comet’s tail will be measured to have a higher flux than the other surrounding sections. Sonnett et al. (2011) used this technique to set a 90% confidence upper limit to the number of Main Belt comets larger than 150 m to be $\sim 400,000$.

Chandler et al. (2021) and Ferellec et al. (2023) used similar azimuthal and coma detection techniques applied to comet candidates observed by the Blanco 4.0-m/Dark Energy Camera and the Isaac Newton Telescope/Wide Field Camera. Chandler et al. (2021) identified activity in asteroid (248370) 2005 QN₁₇₃ using this technique finding evidence of its recurrent activity throughout its orbit. Ferellec et al. (2023) detected an elevated coma and azimuthal asymmetric flux for the Belt asteroid (279870) 2001 NL₁₉ and set an upper limit to the occurrence rate of Main Belt comets of 1:500.

3.3. Detection of cometary activity through sporadic, significant deviations from phase curve brightness

The brightness of asteroids or bare, inactive comet nuclei follow a steady phase function determined by heliocentric, geocentric, and phase angle parameters (Bowell et al., 1988; Muinonen et al., 2010). The phase function predicts an asteroid’s brightness will increase as it gets closer to the Earth, the Sun, and for a smaller phase angle. In general, this phase function is described by a smooth change in brightness for distant asteroids as their

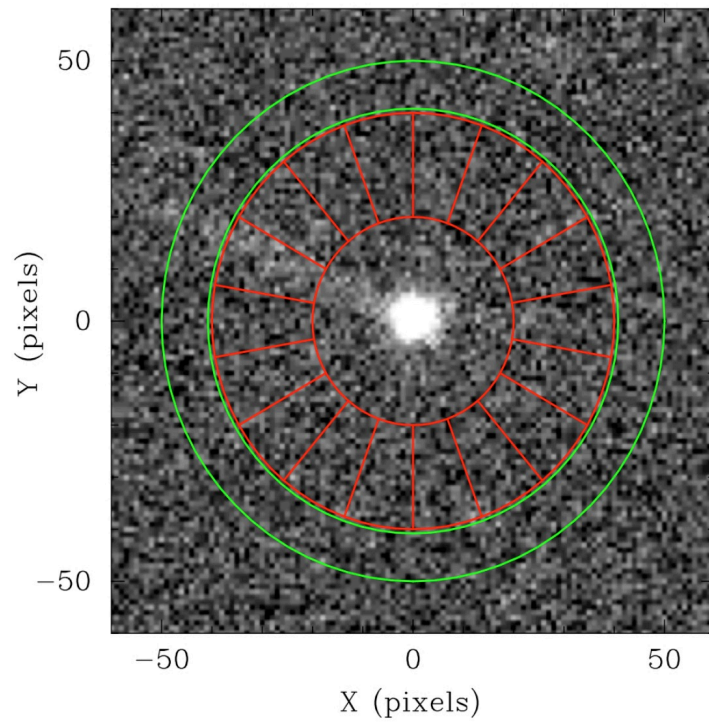


Figure 3: Azimuth scheme for the detection of tails of comets in individual CCD images. The azimuth ring is divided into 18 sections. The section at 10 o'clock encompassing the tail of the detected comet, 133P, measures a higher degree of flux compared to the other sections. The radius of the azimuthal sections was chosen to avoid background stars. Adapted from Figure 2 of Sonnett et al. (2011) and reproduced with the permission of the authors and Icarus.

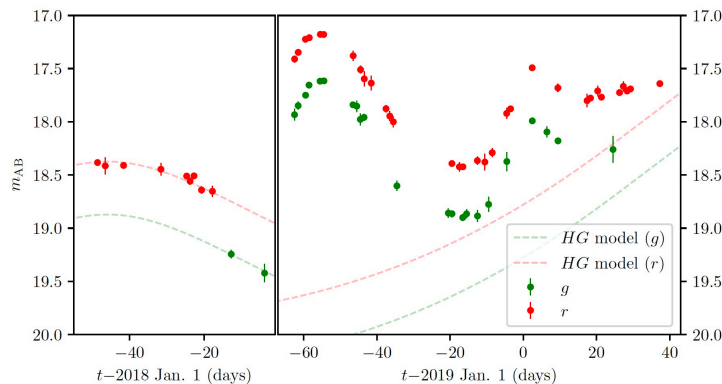


Figure 4: Secular brightness evolution of active asteroid (6478) Gault in 2017-2019. The left and right panels show the evolution in the comet’s brightness (red and green dots) compared to brightness models for a bare nucleus (red and green dashed lines). The brightness evolution of Gault in 2017 follows a typical pattern for a bare nucleus. The brightness pattern significantly deviates and brightens compared to a bare nucleus in 2018-2019. Adapted from Figure 2 of Ye et al. (2019) and reproduced with the permission of the authors and AAS Journals.

viewing geometry changes due to the motion of their orbit and their evolving view from the Earth.

Monitoring the change in brightness of comet candidates with respect to the secular phase function assuming a bare nucleus provides a test of the presence of sudden outbursts or sporadic activity (Kelley et al., 2019). The brightness of a bare nucleus follows a smoothly varying function describing the increase in an object’s brightness as a function of phase angle, heliocentric distance and geocentric distance (Bowell et al., 1988; Muinonen et al., 2010). This technique has been applied to the detection of activity in active asteroid (6478) Gault as seen in Fig. 4 where the brightness of Gault increased by several magnitudes in late 2018/early 2019 ZTF data compared to its phase function (Ye et al., 2019; Purdum et al., 2021). A similar technique was applied to data from ATLAS for the detection of activity in Centaur comets (Dobson et al., 2023).

4. Review of cometary detection methods based on machine learning methods

The next set of methods is based on the growing set of techniques related to Machine Learning (ML). Carruba et al. have already described many of

the core algorithms behind these techniques in Chapter 1 of this volume. We will, therefore, provide an overview of ML-based comet discovery techniques, highlighting where many of these algorithms have been implemented to find comets. Methods such as crowdsourcing used to find comets, while formidable, are outside the scope of this chapter.

4.1. Identification of cometary objects with convolutional neural networks

Fully-connected neural networks (NNs) have been used in machine vision applications such as in image and facial recognition applications (e.g., Bengio, 2009). Applications of NNs adjacent to the recognition of comets include the Morpheus network, a network designed to identify extragalactic sources in *Hubble Space Telescope* image data (Hausen and Robertson, 2020). The training of NNs usually involves training with a gradient descent-like algorithm to converge on minimum-cost function trained model (e.g., Kolen and Kremer, 2001). Fully connected networks are computationally expensive to train and run since they require weights for every hidden layer. However, convolutional neural networks (CNNs) provide a possible workaround by downscaling the first connected layer through convolution and max pooling (see Section 3 of Chapter 1 of this volume for details). This provides an order of magnitude fewer parameters to train and a corresponding considerable speed up in training and reduction in run time while maintaining accurate results compared to fully connected networks.

4.1.1. training of comet identification convolutional neural network models

Previous comet-recognition methods using CNNs relied on a two-stage process combining classical moving object detection methods with CNNs (Chyba Rabeendran and Denneau, 2021). The Tails network by Duev et al. (2021) is the first example to use a CNN trained on comet data to identify comets on a per-image basis. The architecture of the Tails network is provided below in Fig. 5. The training set consisted of $\sim 3,000$ image examples of comets with identifiable cometary morphology; an example can be found in Fig. 6. Each training example consisted of a science image, a reference image consisting of deep stacks of previous images, and an image consisting of the difference between the two. Approximately 20,000 negative examples of point source-like detections, internal reflection artifacts, hot pixels, and diffraction spikes were used as negative examples. The training set was refined with several instances of active learning. Active learning is an interactive form of machine learning in which the user manually labels data to improve the

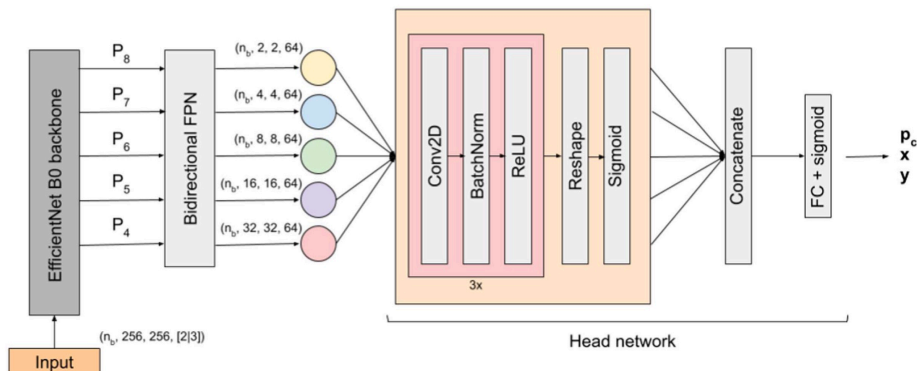


Figure 5: Illustration of the Tails network architecture. Tails uses a combination of bidirectional feature pyramid networks (BiFPN), which are fed by the last five layers of an EfficientDet network. The output of the BiFPN is fed into a head network consisting of several convolutional layers and a fully connected layer and activation function to derive a comet probability score between 0 and 1. Adapted from Fig. 3 of (Duev et al., 2021) and reproduced with the permission of the authors and AAS Journals.

accuracy of a classifier (Fang et al., 2017). In the development of Tails, active learning was used in cases near the network’s decision threshold that were visually inspected, then re-classified and re-added to the revised training set.

4.1.2. Performance of convolutional neural networks to identify comets

The performance of the Tails network with false positive and false negative rates as a function of the comet probability score is shown in Fig. 7; both false positive and false negative rates are below 2%. Tails has been run on the ZTF twilight survey data taken since 2019 September (Bolin et al., 2022a, 2023). The ZTF twilight survey consists of ~ 50 images taken during both evening and morning nautical to astronomical twilight on a nightly basis with Sun-centric distances of 30-60 degrees (Bolin et al., 2022a, 2024a). These near-Sun observations enable the detection of asteroids located inside the orbit of the Earth and Venus as well as of comets (Bolin et al., 2024a). It takes several hours of wall time on a 32-core machine to process a nightly data set. The output with comet probability scores, science, reference, and difference images are output to the Fritz user interface (see Fig. 8) (Coughlin et al., 2023).

The first discovery of a comet made by AI-assisted methods through Tails was made in 2020 October of comet C/2020 T2 (Palomar) as seen in Fig. 9 (Duev et al., 2020). C/2020 T2 exhibits clear cometary features such as a tail

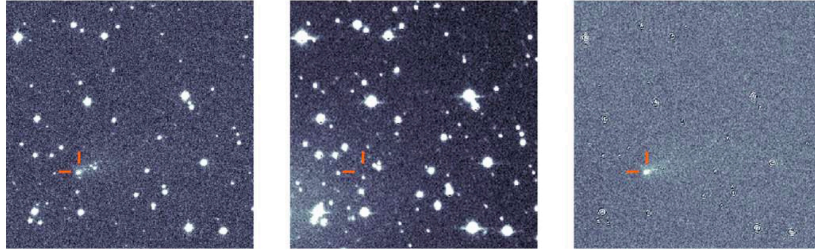


Figure 6: Example of detection of comet C/2019 D1 (Flewelling) used to train the Tails CNN. The left panel shows the science images, the central panel shows the reference panel and the right panel shows the difference between the science and reference image. Adapted from Fig. 2 of (Duev et al., 2021) and reproduced with the permission of the authors and AAS Journals.

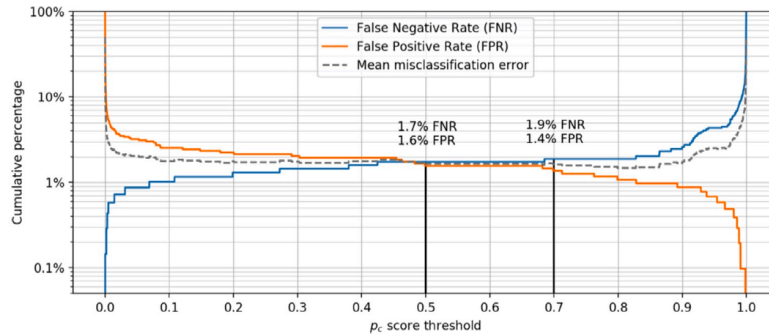


Figure 7: False positive and false negative rates as a function of comet probability score. The False positive and false negative equalize at ~ 1.7 percent for a comet probability score of 0.5 and bifurcate into a false positive rate of ~ 1.4 percent and a false negative rate of ~ 1.9 percent for a score of 0.7. Adapted from Fig. 4 of (Duev et al., 2021) and reproduced with the permission of the authors and AAS Journals.

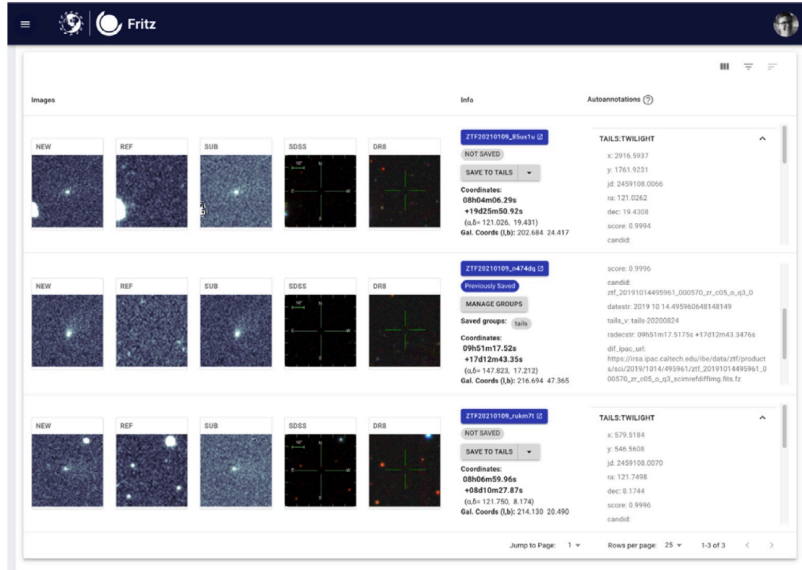


Figure 8: Example Tails interface for the scanning of comet candidates. Adapted from Fig. 5 of (Duez et al., 2021) and reproduced with the permission of the authors and AAS Journals.

and a coma $\sim 3\text{--}4$ arcseconds wide compared to the seeing of ~ 2 arcseconds. In addition to T2, Tails contributed to several other comet discoveries from the ZTF twilight survey, including C/2022 E3 (Bolin et al., 2022b) which will be described in a forthcoming publication (Bolin et al., 2022a, 2024a).

4.2. Other applications of machine learning used to find comets and future developments

Machine learning methods are becoming increasingly used in the detection and discovery of comets that have come out after the development of CNN-based methods like Tails (e.g., Rožek et al., 2023; Sedaghat et al., 2024). Future developments and improvements to CNN-based methods like Tails include the use of multiple-input CNNs, such as the BTSBot, implemented for identifying supernovae in ZTF images (Rehentulla et al., 2023). Multiple input methods combine additional features that can be used to enhance the identification of comets, such as orbital information and PSF-based information described in previous sections. By combining both CNN and other feature information, the accuracy of comet identification can be increased, which will be necessary for future surveys such as LSST.

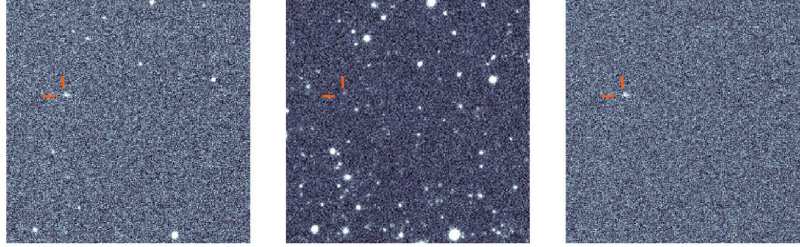


Figure 9: Discovery images of C/2020 T2 (Palomar) taken by ZTF on 2020 October 7. The left panel shows the science image, the center panel shows the reference image and the right panel shows the difference images Adapted from Fig. 7 of (Duev et al., 2021) and reproduced with the permission of the authors and AAS Journals.

Acknowledgments

The authors wish to thank Dr. Valerio Carruba and Dr. Wesley Fraser for providing helpful reviews of this manuscript. Their comments were insightful in the improvement of the manuscript. The authors also wish to thank Ms. Laura-May Abron for her inspiration and artistic insight in the portrayal of ML-methods to identify solar system objects.

References

- Battams, K., Knight, M.M., 2017. SOHO comets: 20 years and 3000 objects later. *Philosophical Transactions of the Royal Society of London Series A* 375, 20160257. doi:10.1098/rsta.2016.0257, arXiv:1611.02279.
- Bauer, J.M., Fernández, Y.R., Protopapa, S., Woodney, L.M., 2022. Comet Science With Ground Based and Space Based Surveys in the New Millennium. arXiv e-prints, arXiv:2210.09400doi:10.48550/arXiv.2210.09400, arXiv:2210.09400.
- Bellm, E.C., Kulkarni, S.R., Graham, M.J., Dekany, R., Smith, R.M., Riddle, R., Masci, F.J., Helou, G., Prince, T.A., Adams, S.M., Barbarino, C., Barlow, T., Bauer, J., Beck, R., Belicki, J., Biswas, R., Blagorodnova, N., Bodewits, D., Bolin, B., Brinnel, V., Brooke, T., Bue, B., Bulla, M., Burruss, R., Cenko, S.B., Chang, C.K., Connolly, A., Coughlin, M., Cromer, J., Cunningham, V., De, K., Delacroix, A., Desai, V., Duev, D.A., Eadie, G., Farnham, T.L., Feeney, M., Feindt, U., Flynn, D., Franckowiak, A., Frederick, S., Fremling, C., Gal-Yam, A., Gezari, S., Giomi, M., Goldstein,

- D.A., Golkhou, V.Z., Goobar, A., Groom, S., Hacopians, E., Hale, D., Henning, J., Ho, A.Y.Q., Hover, D., Howell, J., Hung, T., Huppenkothen, D., Imel, D., Ip, W.H., Ivezić, Ž., Jackson, E., Jones, L., Juric, M., Kasliwal, M.M., Kaspi, S., Kaye, S., Kelley, M.S.P., Kowalski, M., Kramer, E., Kupfer, T., Landry, W., Laher, R.R., Lee, C.D., Lin, H.W., Lin, Z.Y., Lunnan, R., Giomi, M., Mahabal, A., Mao, P., Miller, A.A., Monkewitz, S., Murphy, P., Ngeow, C.C., Nordin, J., Nugent, P., Ofek, E., Patterson, M.T., Penprase, B., Porter, M., Rauch, L., Rebbapragada, U., Reiley, D., Rigault, M., Rodriguez, H., van Roestel, J., Rusholme, B., van Santen, J., Schulze, S., Shupe, D.L., Singer, L.P., Soumagnac, M.T., Stein, R., Surace, J., Sollerman, J., Szkody, P., Taddia, F., Terek, S., Van Sistine, A., van Velzen, S., Vestrand, W.T., Walters, R., Ward, C., Ye, Q.Z., Yu, P.C., Yan, L., Zolkower, J., 2019. The Zwicky Transient Facility: System Overview, Performance, and First Results. *Publications of the Astronomical Society of the Pacific* 131, 018002. doi:10.1088/1538-3873/aaecbe.
- Bengio, Y., 2009. Learning Deep Architectures for AI. *Foundation and Trends in AI* 2, 56.
- Bolin, B., Denneau, L., Micheli, M., Wainscoat, R., Tholen, D.J., Lister, T., Williams, G.V., 2013. Comet P/2013 P5 (Panstarrs). *Central Bureau Electronic Telegrams* 3639.
- Bolin, B.T., Ahumada, T., Dokkum, P.v., Fremling, C., Hardegree-Ullman, K.K., Purdum, J.N., Serabyn, E., Southworth, J., 2023. Preliminary estimates of the Zwicky Transient Facility 'Ayló'chaxnim asteroid population completeness. *Icarus* 394, 115442. doi:10.1016/j.icarus.2023.115442.
- Bolin, B.T., Ahumada, T., van Dokkum, P., Fremling, C., Granvik, M., Hardegree-Ullman, K.K., Harikane, Y., Purdum, J.N., Serabyn, E., Southworth, J., Zhai, C., 2022a. The discovery and characterization of (594913) 'Ayló'chaxnim, a kilometre sized asteroid inside the orbit of Venus. *Monthly Notices of the Royal Astronomical Society* 517, L49–L54. doi:10.1093/mnrasl/slac089, arXiv:2208.07253.
- Bolin, B.T., Delbo, M., Morbidelli, A., Walsh, K.J., 2017. Yarkovsky V-shape identification of asteroid families. *Icarus* 282, 290–312. doi:10.1016/j.icarus.2016.09.029, arXiv:1609.06384.

- Bolin, B.T., Fernandez, Y.R., Lisse, C.M., Holt, T.R., Lin, Z.Y., Purdum, J.N., Deshmukh, K.P., Bauer, J.M., Bellm, E.C., Bodewits, D., Burdge, K.B., Carey, S.J., Copperwheat, C.M., Helou, G., Ho, A.Y.Q., Horner, J., van Roestel, J., Bhalerao, V., Chang, C.K., Chen, C., Hsu, C.Y., Ip, W.H., Kasliwal, M.M., Masci, F.J., Ngeow, C.C., Quimby, R., Burruss, R., Coughlin, M., Dekany, R., Delacroix, A., Drake, A., Duev, D.A., Graham, M., Hale, D., Kupfer, T., Laher, R.R., Mahabal, A., Mróz, P.J., Neill, J.D., Riddle, R., Rodriguez, H., Smith, R.M., Soumagnac, M.T., Walters, R., Yan, L., Zolkower, J., 2021. Initial Characterization of Active Transitioning Centaur, P/2019 LD₂ (ATLAS), Using Hubble, Spitzer, ZTF, Keck, Apache Point Observatory, and GROWTH Visible and Infrared Imaging and Spectroscopy. *Astronomical Journal* 161, 116. doi:10.3847/1538-3881/abd94b, arXiv:2011.03782.
- Bolin, B.T., Fremling, C., Holt, T.R., Hankins, M.J., Ahumada, T., Anand, S., Bhalerao, V., Burdge, K.B., Copperwheat, C.M., Coughlin, M., Deshmukh, K.P., De, K., Kasliwal, M.M., Morbidelli, A., Purdum, J.N., Quimby, R., Bodewits, D., Chang, C.K., Ip, W.H., Hsu, C.Y., Laher, R.R., Lin, Z.Y., Lisse, C.M., Masci, F.J., Ngeow, C.C., Tan, H., Zhai, C., Burruss, R., Dekany, R., Delacroix, A., Duev, D.A., Graham, M., Hale, D., Kulkarni, S.R., Kupfer, T., Mahabal, A., Mróz, P.J., Neill, J.D., Riddle, R., Rodriguez, H., Smith, R.M., Soumagnac, M.T., Walters, R., Yan, L., Zolkower, J., 2020. Characterization of Temporarily Captured Minimoons 2020 CD₃ by Keck Time-resolved Spectrophotometry. *Astrophysical Journal Letters* 900, L45. doi:10.3847/2041-8213/abae69, arXiv:2008.05384.
- Bolin, B.T., Lisse, C.M., 2020. Constraints on the spin-pole orientation, jet morphology, and rotation of interstellar comet 2I/Borisov with deep HST imaging. *Monthly Notices of the Royal Astronomical Society* 497, 4031–4041. doi:10.1093/mnras/staa2192, arXiv:1912.07386.
- Bolin, B.T., Masci, F.J., Coughlin, M.W., Duev, D.W., Stubbs, C.W., 2024a. An artificial-intelligence powered twilight survey of 'Ayló'chaxnim, Atiras, and comets at Palomar Observatory. *Icarus*, submitted. .
- Bolin, B.T., Masci, F.J., Duev, D.A., Milburn, J.W., Neill, J.D., Purdum, J.N., Avdellidou, C., Saki, M., Cheng, Y.C., Delbo, M., Fremling, C.,

- Ghosal, M., Lin, Z.Y., Lisse, C.M., Mahabal, A., 2024b. Palomar discovery and initial characterization of naked-eye long-period comet C/2022 E3 (ZTF). *Monthly Notices of the Royal Astronomical Society* 527, L42–L46. doi:10.1093/mnrasl/slad139, arXiv:2309.14336.
- Bolin, B.T., Masci, F.J., Ip, W.H., Helou, G., Kramer, E.A., Lin, Z.Y., Prince, T.A., Sato, H., Paul, N., Yoshimoto, K., Urbanik, M., Denneau, L., Siverd, R., Tonry, J., Weiland, H., Erasmus, N., Fitzsimmons, A., Lawrence, A., Robinson, J., Siverd, R., Tonry, J., Birtwhistle, P., Jacques, C., Hug, G., Korlevic, K., Buzzi, L., Bacci, R., van Buitenen, G., Buczynski, D., Hale, A., Masek, M., Guido, E., Rocchetto, M., Bryssinck, E., Milani, G., Savini, G., Valvasori, A., Ligustri, R., Bacci, P., Maestripieri, M., Tesi, L., Fagioli, G., Lutkenhoner, B., 2022b. Comet C/2022 E3 (ZTF). *Minor Planet Electronic Circulars* 2022-F13.
- Bolin, B.T., Morbidelli, A., Walsh, K.J., 2018. Size-dependent modification of asteroid family Yarkovsky V-shapes. *Astronomy & Astrophysics* 611, A82. doi:10.1051/0004-6361/201732079, arXiv:1710.04208.
- Born, M., Wolf, E., 1999. *Principles of Optics*.
- Bowell, E., Hapke, B., Domingue, D., Lumme, K., Peltoniemi, J., Harris, A., 1988. Application of Photometric Models to Asteroids. *Asteroids II*, 399–433.
- Chambers, K.C., Magnier, E.A., Metcalfe, N., Flewelling, H.A., Huber, M.E., Waters, C.Z., Denneau, L., Draper, P.W., Farrow, D., Finkbeiner, D.P., Holmberg, C., Koppenhoefer, J., Price, P.A., Saglia, R.P., Schlafly, E.F., Smartt, S.J., Sweeney, W., Wainscoat, R.J., Burgett, W.S., Grav, T., Heasley, J.N., Hodapp, K.W., Jedicke, R., Kaiser, N., Kudritzki, R.P., Luppino, G.A., Lupton, R.H., Monet, D.G., Morgan, J.S., Onaka, P.M., Stubbs, C.W., Tonry, J.L., Banados, E., Bell, E.F., Bender, R., Bernard, E.J., Botticella, M.T., Casertano, S., Chastel, S., Chen, W.P., Chen, X., Cole, S., Deacon, N., Frenk, C., Fitzsimmons, A., Gezari, S., Goessl, C., Goggia, T., Goldman, B., Grebel, E.K., Hambly, N.C., Hasinger, G., Heavens, A.F., Heckman, T.M., Henderson, R., Henning, T., Holman, M., Hopp, U., Ip, W.H., Isani, S., Keyes, C.D., Koekemoer, A., Kotak, R., Long, K.S., Lucey, J.R., Liu, M., Martin, N.F., McLean, B., Morganson, E., Murphy, D.N.A., Nieto-Santisteban, M.A., Norberg, P., Peacock, J.A.,

- Pier, E.A., Postman, M., Primak, N., Rae, C., Rest, A., Riess, A., Riffeser, A., Rix, H.W., Roser, S., Schilbach, E., Schultz, A.S.B., Scolnic, D., Szalay, A., Seitz, S., Shiao, B., Small, E., Smith, K.W., Soderblom, D., Taylor, A.N., Thakar, A.R., Thiel, J., Thilker, D., Urata, Y., Valenti, J., Walter, F., Watters, S.P., Werner, S., White, R., Wood-Vasey, W.M., Wyse, R., 2016. The Pan-STARRS1 Surveys. ArXiv e-prints [arXiv:1612.05560](https://arxiv.org/abs/1612.05560).
- Chandler, C.O., Trujillo, C.A., Hsieh, H.H., 2021. Recurrent Activity from Active Asteroid (248370) 2005 QN₁₇₃: A Main-belt Comet. *Astrophysical Journal Letters* 922, L8. doi:[10.3847/2041-8213/ac365b](https://doi.org/10.3847/2041-8213/ac365b), [arXiv:2111.06405](https://arxiv.org/abs/2111.06405).
- Cheng, Y.C., Wu, Y.L., 2022. Cometary Activities of the Hyperbolic Asteroid A/2021 X2 Observed at Lulin Observatory. *The Astronomer's Telegram* 15597, 1.
- Chyba Rabeendran, A., Denneau, L., 2021. A Two-stage Deep Learning Detection Classifier for the ATLAS Asteroid Survey. *Publications of the Astronomical Society of the Pacific* 133, 034501. doi:[10.1088/1538-3873/abc900](https://doi.org/10.1088/1538-3873/abc900), [arXiv:2101.08912](https://arxiv.org/abs/2101.08912).
- Coughlin, M.W., Bloom, J.S., Nir, G., Antier, S., du Laz, T.J., van der Walt, S., Crellin-Quick, A., Culino, T., Duev, D.A., Goldstein, D.A., Healy, B.F., Karambelkar, V., Lilleboe, J., Shin, K.M., Singer, L.P., Ahumada, T., Anand, S., Bellm, E.C., Dekany, R., Graham, M.J., Kasliwal, M.M., Kostadinova, I., Kiendrebeogo, R.W., Kulkarni, S.R., Jenkins, S., LeBaron, N., Mahabal, A.A., Neill, J.D., Parazin, B., Peloton, J., Perley, D.A., Riddle, R., Rusholme, B., van Santen, J., Sollerman, J., Stein, R., Turpin, D., Wold, A., Amat, C., Bonneau, A., Bonnefoy, A., Flament, M., Kerkow, F., Kishore, S., Jani, S., Mahanty, S.K., Liu, C., Llinares, L., Makarison, J., Olli eric, A., Perez, I., Pont, L., Sharma, V., 2023. A Data Science Platform to Enable Time-domain Astronomy. *Astrophysical Journal Supplement* 267, 31. doi:[10.3847/1538-4365/acdee1](https://doi.org/10.3847/1538-4365/acdee1), [arXiv:2305.00108](https://arxiv.org/abs/2305.00108).
- Denneau, L., Jedicke, R., Grav, T., Granvik, M., Kubica, J., Milani, A., Vereš, P., Wainscoat, R., Chang, D., Pierfederici, F., Kaiser, N., Chambers, K.C., Heasley, J.N., Magnier, E.A., Price, P.A., Myers, J., Kleyna, J., Hsieh, H., Farnocchia, D., Waters, C., Sweeney, W.H., Green, D., Bolin,

- B., Burgett, W.S., Morgan, J.S., Tonry, J.L., Hodapp, K.W., Chastel, S., Chesley, S., Fitzsimmons, A., Holman, M., Spahr, T., Tholen, D., Williams, G.V., Abe, S., Armstrong, J.D., Bressi, T.H., Holmes, R., Lister, T., McMillan, R.S., Micheli, M., Ryan, E.V., Ryan, W.H., Scotti, J.V., 2013. The Pan-STARRS Moving Object Processing System. *Publications of the Astronomical Society of the Pacific* 125, 357–395. doi:10.1086/670337, arXiv:1302.7281.
- Dobson, M.M., Schwamb, M.E., Benecchi, S.D., Verbiscer, A.J., Fitzsimmons, A., Shingles, L.J., Denneau, L., Heinze, A.N., Smith, K.W., Tonry, J.L., Weiland, H., Young, D.R., 2023. Phase Curves of Kuiper Belt Objects, Centaurs, and Jupiter-family Comets from the ATLAS Survey. *Planetary Science Journal* 4, 75. doi:10.3847/PSJ/acc463, arXiv:2303.08643.
- Duev, D.A., Bolin, B.T., Graham, M.J., Kelley, M.S.P., Mahabal, A., Bellm, E.C., Coughlin, M.W., Dekany, R., Helou, G., Kulkarni, S.R., Masci, F.J., Prince, T.A., Riddle, R., Soumagnac, M.T., van der Walt, S.J., 2021. Tails: Chasing Comets with the Zwicky Transient Facility and Deep Learning. *Astronomical Journal* 161, 218. doi:10.3847/1538-3881/abea7b, arXiv:2102.13352.
- Duev, D.A., Duev, I.D., Bolin, B.T., 2020. COMET C/2020 T2 (Palomar). *Minor Planet Electronic Circulars* 2020-U170.
- Duev, D.A., Mahabal, A., Ye, Q., Tirumala, K., Belicki, J., Dekany, R., Frederick, S., Graham, M.J., Laher, R.R., Masci, F.J., Prince, T.A., Riddle, R., Rosnet, P., Soumagnac, M.T., 2019. DeepStreaks: identifying fast-moving objects in the Zwicky Transient Facility data with deep learning. *Monthly Notices of the Royal Astronomical Society* 486, 4158–4165. doi:10.1093/mnras/stz1096, arXiv:1904.05920.
- Fang, M., Li, Y., Cohn, T., 2017. Learning how to Active Learn: A Deep Reinforcement Learning Approach, in: *Proceedings of the 2017 Conference on Empirical Methods in Natural Language Processing*, Association for Computational Linguistics, Copenhagen, Denmark. pp. 595–605.
- Ferellec, L., Snodgrass, C., Fitzsimmons, A., Rožek, A., Gardener, D., Smith, R., Medeiros, H., Opitom, C., Hsieh, H.H., 2023. A targeted search for

- Main Belt Comets. *Monthly Notices of the Royal Astronomical Society* 518, 2373–2384. doi:10.1093/mnras/stac3199, arXiv:2211.01435.
- Festou, M.C., Rickman, H., West, R.M., 1993. Comets. *Astronomy and Astrophysics Review* 4, 363–447. doi:10.1007/BF00872944.
- Fraser, W.C., Dones, L., Volk, K., Womack, M., Nesvorný, D., 2022. The Transition from the Kuiper Belt to the Jupiter-Family (Comets). arXiv e-prints , arXiv:2210.16354doi:10.48550/arXiv.2210.16354, arXiv:2210.16354.
- Gladman, B., Marsden, B.G., Vanlaerhoven, C., 2008. Nomenclature in the Outer Solar System, in: Barucci, M.A., Boehnhardt, H., Cruikshank, D.P., Morbidelli, A., Dotson, R. (Eds.), *The Solar System Beyond Neptune*, pp. 43–57.
- Hausen, R., Robertson, B.E., 2020. Morpheus: A Deep Learning Framework for the Pixel-level Analysis of Astronomical Image Data. *Astrophysical Journal Supplement* 248, 20. doi:10.3847/1538-4365/ab8868, arXiv:1906.11248.
- Hill, R.E., Bolin, B., Kleyna, J., Denneau, L., Wainscoat, R., Micheli, M., Armstrong, J.D., Molina, M., Sato, H., 2013. Comet P/2013 R3 (Catalina-Panstarrs). *Central Bureau Electronic Telegrams* 3658.
- Howell, S.B., 2000. *Handbook of CCD Astronomy*.
- Hsieh, H.H., Denneau, L., Wainscoat, R.J., Schörghofer, N., Bolin, B., Fitzsimmons, A., Jedicke, R., Kleyna, J., Micheli, M., Vereš, P., Kaiser, N., Chambers, K.C., Burgett, W.S., Flewelling, H., Hodapp, K.W., Magnier, E.A., Morgan, J.S., Price, P.A., Tonry, J.L., Waters, C., 2015. The main-belt comets: The Pan-STARRS1 perspective. *Icarus* 248, 289–312. doi:10.1016/j.icarus.2014.10.031, arXiv:1410.5084.
- Jedicke, R., Bolin, B., Granvik, M., Beshore, E., 2016. A fast method for quantifying observational selection effects in asteroid surveys. *Icarus* 266, 173–188. doi:10.1016/j.icarus.2015.10.021.
- Jedicke, R., Granvik, M., Micheli, M., Ryan, E., Spahr, T., Yeomans, D.K., 2015. Surveys, Astrometric Follow-Up, and Population Statistics. *Asteroids IV* , 795–813.

- Jedicke, R., Larsen, J., Spahr, T., 2002. Observational Selection Effects in Asteroid Surveys. *Asteroids III*, 71–87.
- Kelley, M.S.P., Bodewits, D., Ye, Q., Laher, R.R., Masci, F.J., Monkewitz, S., Riddle, R., Rusholme, B., Shupe, D.L., Soumagnac, M.T., 2019. ZChecker: Finding Cometary Outbursts with the Zwicky Transient Facility, in: Teuben, P.J., Pound, M.W., Thomas, B.A., Warner, E.M. (Eds.), *Astronomical Data Analysis Software and Systems XXVII*, p. 471.
- Kolen, J.F., Kremer, S.C., 2001. Gradient Flow in Recurrent Nets: The Difficulty of Learning Long-Term Dependencies. pp. 237–243. doi:10.1109/9780470544037.ch14.
- Kubica, J., Moore, A., Connolly, A., Jedicke, R., 2005. Efficiently identifying close track/observation pairs in continuous timed data, SPIE.
- Mainzer, A., Bauer, J., Grav, T., Masiero, J., Cutri, R.M., Dailey, J., Eisenhardt, P., McMillan, R.S., Wright, E., Walker, R., Jedicke, R., Spahr, T., Tholen, D., Alles, R., Beck, R., Brandenburg, H., Conrow, T., Evans, T., Fowler, J., Jarrett, T., Marsh, K., Masci, F., McCallon, H., Wheelock, S., Wittman, M., Wyatt, P., DeBaun, E., Elliott, G., Elsbury, D., Gautier, IV, T., Gomillion, S., Leisawitz, D., Maleszewski, C., Micheli, M., Wilkins, A., 2011. Preliminary Results from NEOWISE: An Enhancement to the Wide-field Infrared Survey Explorer for Solar System Science. *ApJ* 731, 53. doi:10.1088/0004-637X/731/1/53, arXiv:1102.1996.
- Masci, F.J., Laher, R.R., Rusholme, B., Shupe, D.L., Groom, S., Surace, J., Jackson, E., Monkewitz, S., Beck, R., Flynn, D., Terek, S., Landry, W., Hacopians, E., Desai, V., Howell, J., Brooke, T., Imel, D., Wachter, S., Ye, Q.Z., Lin, H.W., Cenko, S.B., Cunningham, V., Rebbapragada, U., Bue, B., Miller, A.A., Mahabal, A., Bellm, E.C., Patterson, M.T., Jurić, M., Golkhou, V.Z., Ofek, E.O., Walters, R., Graham, M., Kasliwal, M.M., Dekany, R.G., Kupfer, T., Burdge, K., Cannella, C.B., Barlow, T., Van Sistine, A., Giomi, M., Fremling, C., Blagorodnova, N., Levitan, D., Riddle, R., Smith, R.M., Helou, G., Prince, T.A., Kulkarni, S.R., 2019. The Zwicky Transient Facility: Data Processing, Products, and Archive. *Publications of the Astronomical Society of the Pacific* 131, 018003. doi:10.1088/1538-3873/aae8ac, arXiv:1902.01872.

- Masiero, J., Jedicke, R., Ďurech, J., Gwyn, S., Denneau, L., Larsen, J., 2009. The Thousand Asteroid Light Curve Survey. *Icarus* 204, 145–171. doi:10.1016/j.icarus.2009.06.012, arXiv:0906.3339.
- Muinenen, K., Belskaya, I.N., Cellino, A., Delbò, M., Levasseur-Regourd, A.C., Penttilä, A., Tedesco, E.F., 2010. A three-parameter magnitude phase function for asteroids. *Icarus* 209, 542–555. doi:10.1016/j.icarus.2010.04.003.
- Nesvorný, D., Deienno, R., Bottke, W.F., Jedicke, R., Naidu, S., Chesley, S.R., Chodas, P.W., Granvik, M., Vokrouhlický, D., Brož, M., Morbidelli, A., Christensen, E., Shelly, F.C., Bolin, B.T., 2023. NEOMOD: A New Orbital Distribution Model for Near-Earth Objects. *Astronomical Journal* 166, 55. doi:10.3847/1538-3881/ace040, arXiv:2306.09521.
- Purdum, J.N., Lin, Z.Y., Bolin, B.T., Sharma, K., Choi, P.I., Bhalerao, V., Hanuš, J., Kumar, H., Quimby, R., van Roestel, J.C., Zhai, C., Fernandez, Y.R., Lisse, C.M., Bodewits, D., Fremling, C., Ryan Golovich, N., Hsu, C.Y., Ip, W.H., Ngeow, C.C., Saini, N.S., Shao, M., Yao, Y., Ahumada, T., Anand, S., Andreoni, I., Burdge, K.B., Burruss, R., Chang, C.K., Copperwheat, C.M., Coughlin, M., De, K., Dekany, R., Delacroix, A., Drake, A., Duev, D., Graham, M., Hale, D., Kool, E.C., Kasliwal, M.M., Kostadinova, I.S., Kulkarni, S.R., Laher, R.R., Mahabal, A., Masci, F.J., Mróz, P.J., Neill, J.D., Riddle, R., Rodriguez, H., Smith, R.M., Walters, R., Yan, L., Zolkower, J., 2021. Time-series and Phase-curve Photometry of the Episodically Active Asteroid (6478) Gault in a Quiescent State Using APO, GROWTH, P200, and ZTF. *Astrophysical Journal Letters* 911, L35. doi:10.3847/2041-8213/abf2ca, arXiv:2102.13017.
- Rehemtulla, N., Miller, A.A., Coughlin, M.W., Jegou du Laz, T., 2023. BTSbot: A Multi-input Convolutional Neural Network to Automate and Expedite Bright Transient Identification for the Zwicky Transient Facility. arXiv e-prints , arXiv:2307.07618doi:10.48550/arXiv.2307.07618, arXiv:2307.07618.
- Rožek, A., Snodgrass, C., Jørgensen, U.G., Pravec, P., Bonavita, M., Rabus, M., Khalouei, E., Longa-Peña, P., Burgdorf, M.J., Donaldson, A., Gardener, D., Crake, D., Sajadian, S., Bozza, V., Skottfelt, J., Dominik, M., Fynbo, J., Hinse, T.C., Hundertmark, M., Rahvar, S., Southworth, J.,

- Tregloan-Reed, J., Kretlow, M., Rota, P., Peixinho, N., Andersen, M., Amadio, F., Barrios-López, D., Castillo Baeza, N.S., 2023. Optical Monitoring of the Didymos-Dimorphos Asteroid System with the Danish Telescope around the DART Mission Impact. *Planetary Science Journal* 4, 236. doi:10.3847/PSJ/ad0a64, arXiv:2311.01982.
- Sato, H., Yoshimoto, K., Guido, E., Nakano, S., 2022. COMET C/2022 E3. CBET 5111.
- Schwamb, M.E., Jones, R.L., Yoachim, P., Volk, K., Dorsey, R.C., Opitom, C., Greenstreet, S., Lister, T., Snodgrass, C., Bolin, B.T., Inno, L., Bannister, M.T., Eggl, S., Solontoi, M., Kelley, M.S.P., Jurić, M., Lin, H.W., Ragozzine, D., Bernardinelli, P.H., Chesley, S.R., Daylan, T., Ďurech, J., Fraser, W.C., Granvik, M., Knight, M.M., Lisse, C.M., Malhotra, R., Oldroyd, W.J., Thirouin, A., Ye, Q., 2023. Tuning the Legacy Survey of Space and Time (LSST) Observing Strategy for Solar System Science. *Astrophysical Journal Supplement* 266, 22. doi:10.3847/1538-4365/acc173, arXiv:2303.02355.
- Scotti, J.V., Gehrels, T., Rabinowitz, D.L., 1992. Automated Detection of Asteroids in Real-Time with the Spacewatch Telescope, in: Harris, A.W., Bowell, E. (Eds.), *Asteroids, Comets, Meteors 1991*, p. 541.
- Sedaghat, N., Chandler, C.O., Oldroyd, W.J., Trujillo, C.A., Burris, W.A., Hsieh, H.H., Kueny, J.K., Farrell, K.A., DeSpain, J.A., Magbanua, M.J.M., Sheppard, S.S., Mazzucato, M.T., Bosch, M.K.D., Shaw-Diaz, T., Gonano, V., Lamperti, A., da Silva Campos, J.A., Goodwin, B.L., Terentev, I.A., Dukes, C.J.A., 2024. 2016 UU121: An Active Asteroid Discovery via AI-enhanced Citizen Science. *Research Notes of the American Astronomical Society* 8, 51. doi:10.3847/2515-5172/ad2b66.
- Sonnett, S., Kleyana, J., Jedicke, R., Masiero, J., 2011. Limits on the size and orbit distribution of main belt comets. *Icarus* 215, 534–546. doi:10.1016/j.icarus.2011.08.001, arXiv:1108.3095.
- Tonry, J.L., Denneau, L., Heinze, A.N., Stalder, B., Smith, K.W., Smartt, S.J., Stubbs, C.W., Weiland, H.J., Rest, A., 2018. ATLAS: A High-cadence All-sky Survey System. *Publications of the Astronomical Society of the Pacific* 130, 064505. doi:10.1088/1538-3873/aabadf, arXiv:1802.00879.

- Waszczak, A., Ofek, E.O., Aharonson, O., Kulkarni, S.R., Polishook, D., Bauer, J.M., Levitan, D., Sesar, B., Laher, R., Surace, J., PTF Team, 2013. Main-belt comets in the Palomar Transient Factory survey - I. The search for extendedness. *Monthly Notices of the Royal Astronomical Society* 433, 3115–3132. doi:10.1093/mnras/stt951, arXiv:1305.7176.
- Whidden, P.J., Bryce Kalmbach, J., Connolly, A.J., Jones, R.L., Smotherman, H., Bektesevic, D., Slater, C., Becker, A.C., Ivezić, Ž., Jurić, M., Bolin, B., Moeyens, J., Förster, F., Golkhou, V.Z., 2019. Fast Algorithms for Slow Moving Asteroids: Constraints on the Distribution of Kuiper Belt Objects. *Astronomical Journal* 157, 119. doi:10.3847/1538-3881/aafd2d, arXiv:1901.02492.
- Ye, Q., Kelley, M.S.P., Bodewits, D., Bolin, B., Jones, L., Lin, Z.Y., Bellm, E.C., Dekany, R., Duev, D.A., Groom, S., Helou, G., Kulkarni, S.R., Kupfer, T., Masci, F.J., Prince, T.A., Soumagnac, M.T., 2019. Multiple Outbursts of Asteroid (6478) Gault. *Astrophysical Journal Letters* 874, L16. doi:10.3847/2041-8213/ab0f3c, arXiv:1903.05320.